Earth and Planetary Science Letters 275 (2008) 102–110

Contents lists available at ScienceDirect

Earth and Planetary Science Letters

journal homepage: www.elsevier.com/locate/epsl

Post-depositional remanent magnetization lock-in and the location of the Matuyama–Brunhes geomagnetic reversal boundary in marine and Chinese loess sequences

Qingsong Liu [a,b,*], Andrew P. Roberts [b], Eelco J. Rohling [b], Rixiang Zhu [a], Youbin Sun [c]

[a] Paleomagnetism and Geochronology Laboratory (SKL-LE), Institute of Geology and Geophysics, Chinese Academy of Sciences, Beijing 100029, People's Republic of China
[b] National Oceanography Centre, University of Southampton, European Way, Southampton SO14 3ZH, UK
[c] State Key Laboratory of Loess and Quaternary Geology, Institute of Earth Environment, Chinese Academy of Sciences, Xi'an 710075, People's Republic of China

ARTICLE INFO

Article history:
Received 9 January 2008
Received in revised form 26 July 2008
Accepted 6 August 2008
Available online 18 September 2008

Editor: M.L. Delaney

Keywords:
Matuyama–Brunhes boundary
marine sediment
post-depositional remanent magnetization (PDRM)
lock-in
loess
paleosol

ABSTRACT

Bioturbation disturbs detrital magnetic particles after deposition, so accurate recording of the ancient geomagnetic field in bioturbated sediments is widely attributed to acquisition of a post-depositional remanent magnetization (PDRM) whereby the geomagnetic field exerts a torque on a magnetic particle and aligns it with the field after the final mixing event experienced by the particle. The relationship between the Matuyama–Brunhes boundary (MBB) and oxygen isotope age tie points in marine sediments has been widely used to determine the depth at which the paleomagnetic signal is locked-in. However, such analyses can be badly affected by age discrepancies among different paleoclimatic proxies and by varying isotopic compositions of seawater in different locations and from the presence of different water masses at different depths at the same location. It is therefore necessary to separately compare paleomagnetic data with respect to either benthic or planktonic foraminiferal oxygen isotope records for sites from the same water mass to avoid inadvertently introducing age differences to the analysis. When the global data set is subjected to such a rigorous analysis, few reliable data remain for the MBB. Using two complementary approaches, we estimate that the MBB is, on average, shifted ≤20 cm below its true position in marine sediments. This offset is the sum of the thickness of the bioturbated surface mixed layer, which is possibly dominant, and the PDRM lock-in depth. There is also controversy concerning observed differences in the position of the MBB relative to paleoclimatic proxies in marine sediments and Chinese loess deposits. For the Chinese loess, quartz grain size is insensitive to pedogenic alteration and is a useful parameter for determining the true position of the MBB with respect to paleoclimatic boundaries. We conclude that the MBB occurs late in marine oxygen isotope stage 19, and in the upper part of Chinese paleosol unit S8, rather than at the mid or lower part of loess unit L8. Our results require adjustment of the generally accepted positions for the MBB, and resolve a longstanding chronological conundrum for marine and Chinese loess sequences.

© 2008 Elsevier B.V. All rights reserved.

1. Introduction

Despite the fact that sedimentary magnetizations have been widely analysed in paleomagnetic studies over the last 60 yr, considerable debate remains concerning the mechanism(s) by which sediments become magnetized. Bioturbation disturbs detrital magnetic particles after deposition, so accurate recording of the ancient geomagnetic field in bioturbated sediments is widely attributed to acquisition of a post-depositional remanent magnetization (PDRM) (Kent, 1973; Verosub, 1977; Hyodo, 1984; Bleil and von Dobeneck, 1999; Roberts and Winklhofer, 2004). A PDRM will only be recorded once a magnetic particle has passed through a surface mixed layer (SML) and an underlying lock-in zone. The thickness of the SML typically ranges from several cm to several tens of cm in marine sediments and, on average, is estimated to be ~10 cm (Boudreau, 1994, 1998). The downward offset of a sedimentary paleomagnetic record will therefore be the sum of the SML thickness and the lock-in depth (e.g., Channell and Kleiven, 2000; Channell and Guyodo, 2004; Roberts and Winklhofer, 2004). However, the physical effects of mixing and lock-in are markedly different. The SML will simply shift the paleomagnetic record downward without necessarily filtering the signal. In contrast, lock-in processes serve as a low-band pass filter and high-frequency features will be filtered out even for relatively shallow lock-in depths (Hyodo, 1984; Roberts and Winklhofer, 2004).

The last geomagnetic reversal, the Matuyama–Brunhes boundary (MBB), is an important chronological marker in both marine sediments and in wind-blown Chinese loess/paleosol deposits. However, there remain arguments about the exact stratigraphic location of the MBB as recorded in both Chinese loess and marine

* Corresponding author. Paleomagnetism and Geochronology Laboratory (SKL-LE), Institute of Geology and Geophysics, Chinese Academy of Sciences, Beijing 100029, People's Republic of China.
E-mail address: liux0272@yahoo.com (Q. Liu).

0012-821X/$ – see front matter © 2008 Elsevier B.V. All rights reserved.
doi:10.1016/j.epsl.2008.08.004

sediments; the associated uncertainties have hindered accurate correlation between these important paleoclimatic archives (e.g., Tauxe et al., 1996; Zhou and Shackleton, 1999; Guo et al., 2001).

In Chinese loess sequences, the MBB has been detected in either the middle or at the bottom of loess unit L8, which formed during a glacial period (Heller et al., 1987; Kukla and An, 1989; Zheng et al., 1992; Zhu et al., 1994; Spassov et al., 2003). However, in marine sediments, the MBB is recorded in an interglacial period during marine oxygen isotope stage (MIS) 19 (Tauxe et al., 1996). This glacial versus interglacial discrepancy has been attributed to different PDRM lock-in depths in different environments and to bioturbation within the SML, although a paleoclimatic phase lag between Chinese loess and marine sediments has also been proposed (Forster and Heller, 1994; Zhu et al., 1998).

In this study, we first provide a mechanism to explain the apparent chronostratigraphic variability of the MBB by looking in more detail at paleoclimatic proxies from Chinese loess sequences. Second, we focus on 'benthic–benthic' and 'planktonic–planktonic' correlations of foraminiferal $\delta^{18}O$ records for marine cores from similar hydrographic settings to avoid potential problems that have affected previous analyses of PDRM lock-in. Our aim is to test the robustness of conclusions drawn from previous studies and to resolve the problem concerning the position of the MBB, which will assist with correlation of paleoclimate records from marine sediments and Chinese loess/paleosol sequences.

2. Previous estimates of PDRM lock-in and the position of the MBB

deMenocal et al. (1990) reported that the stratigraphic location of the MBB within marine sediments in MIS 19 is a function of sediment accumulation rate (SAR). When the SAR is larger than ~1 cm/kyr, the downward offset of the MBB with respect to $\delta^{18}O$ datums is linearly correlated to SAR. deMenocal et al. (1990) estimated that the MBB was locked-in about 16 cm below the contemporaneous sediment surface. Much larger depth offsets (~30–50 cm) occurred for SAR less than ~1 cm/kyr, as revealed by the large vertical dispersion of microtektite layers. deMenocal et al. (1990) suggested that these sediments have unusual physical properties and did not include them in his analysis.

In contrast to deMenocal et al. (1990), Tauxe et al. (1996) compiled 19 marine records for the MBB and concluded that there are no apparent displacements of the MBB within MIS 19 and that the combined effects of PDRM lock-in and surficial mixing are weak in marine carbonate sediments. Tauxe et al. (1996) therefore proposed that the MBB recorded in Chinese loess unit L8 must have been shifted downward from the overlying paleosol unit S7 in order to resolve the problem of the glacial versus interglacial position for the MBB in the Chinese loess. In this case, paleosol S7, rather than S8, would correspond to MIS 19. Zhou and Shackleton (1999) then examined the stratigraphic location of microtektites in relation to the stratigraphic position of the MBB in the Chinese loess sequences. They reinforced the idea of Tauxe et al. (1996) that the MBB recorded by the Chinese loess has been displaced downward by about 2–3 m (equivalent to about 20–30 ka), and that units S7 and L8 should be directly correlated to MIS 19 and 20, respectively. Heslop et al. (2000) developed a new astronomical time scale for Chinese loess sequences using this relationship and the 2–3 m lock-in proposed by Zhou and Shackleton (1999). To account for the possible large downward shift of the MBB in Chinese loess sequences, while enabling recording of some high-frequency geomagnetic features, Spassov et al. (2003) developed a composite model in which the natural remanent magnetization (NRM) is a shallow PDRM that is augmented by a later pedogenic chemical remanent magnetization (CRM).

The approaches used by both deMenocal et al. (1990) and Tauxe et al. (1996) are theoretically feasible, but practical limitations have resulted in opposite conclusions from similar procedures. First, these authors analysed globally distributed marine records. Skinner and Shackleton (2005) found that the MIS 2/1 boundary recorded by benthic foraminiferal $\delta^{18}O$ data in the deep eastern equatorial Pacific Ocean (core TR163-31B) was delayed by about 4 kyr compared to the deep Northeast Atlantic (core MD99-2334K). This offset would seem to be too large to be simply attributed to ocean mixing times. They therefore suggested that local temperature changes in the Pacific Ocean could have significantly affected the benthic foraminiferal $\delta^{18}O$ signal. Caution therefore needs to be exercised when directly comparing $\delta^{18}O$ records for cores from different hydrographic settings because the signals could be diachronous. Second, previous studies used comparisons between different paleoclimatic proxies, e.g., both planktonic and benthic foraminiferal $\delta^{18}O$ data (deMenocal et al., 1990; Tauxe et al., 1996), gamma-ray attenuation porosity evaluator (GRAPE) records for Ocean Drilling Program (ODP) holes 660A, 665A, 804C and 807A (Tauxe et al., 1996), and $CaCO_3$% data for ODP Site 609 (deMenocal et al., 1990). Even planktonic and benthic foraminiferal $\delta^{18}O$ records from a single site might not be perfectly in-phase. For example, Shackleton et al. (2000) documented that benthic and planktonic foraminiferal $\delta^{18}O$ records from a North Atlantic core have completely different patterns (amplitude, phase and even general features) because they record signals associated with different water masses. It is therefore problematical to directly correlate different proxies from different sites. This includes correlation between benthic and planktonic foraminiferal $\delta^{18}O$ records, unless an in-phase relationship can be independently demonstrated for these proxies at each site.

A further impediment to quantifying the relationship between MBB offset and SAR is that designated age tie points can have large relative uncertainties. For example, deMenocal et al. (1990) selected the mid-point of MIS 19 as a reference point, while Tauxe et al. (1996) used MIS 20.2 and 18.4 as their age tie points. For some of the cores used in these studies, e.g., Deep Sea Drilling Project (DSDP) Hole 502B, ODP Site 610 (deMenocal et al., 1990), ERDC103p, ODP 851E, and DSDP 502B (Tauxe et al., 1996), the termination of MIS 19 cannot be well-defined. This is mainly because the shape of MIS 19 differs greatly from core to core. For example, a dominant peak (in an inverted $\delta^{18}O$ scale) was found for cores V28-238, V28-239, M13519, ODP 607A, and ODP 805C and two or more peaks are present in records from DSDP 502B, ODP 610, and ODP 769A (deMenocal et al., 1990; Tauxe et al., 1996). The diverse $\delta^{18}O$ patterns for MIS 19 in different cores may result from different factors at different locations (e.g., ice volume, hydrological budget (salinity), temperature, hydrography, etc.). In addition, bioturbation may have filtered high-frequency features out of some of the $\delta^{18}O$ records. Moreover, the sampling rates in many older studies are low, e.g., only five or six data points define MIS 19 at ODP holes 607A and 785A, which inhibits accurate determination of the stratigraphic location of MIS boundaries in these cores. We therefore conclude that much of the global data used in previous analyses of PDRM lock-in and MBB offsets in marine sediments are not completely adequate for such purposes. Below, we focus on two North Atlantic ODP holes (982C and 983A), and on two sites from the western equatorial Pacific Ocean (V28-238 and V28-239). The cores in each pair are situated (Fig. 1) at similar water depths and within the same water mass, and have different sedimentation rates, which are necessary requirements for our analysis.

3. Position of the MBB in the Chinese loess

Tauxe et al. (1996) and Zhou and Shackleton (1999) proposed a large lock-in depth of about 2–3 m for the MBB in the Chinese loess. Three mechanisms could explain such a large downward displacement of the MBB: 1) large PDRM lock-in effects (Zhou and Shackleton, 1999), 2) delayed acquisition of a chemical remanent magnetization (CRM) (Spassov et al., 2003), and 3) incorrect interpretation of the position of MIS boundaries within the loess sequence based on magnetic susceptibility correlations. The large downward displacement of the MBB (2–3 m) suggested by Zhou and Shackleton (1999) cannot be caused

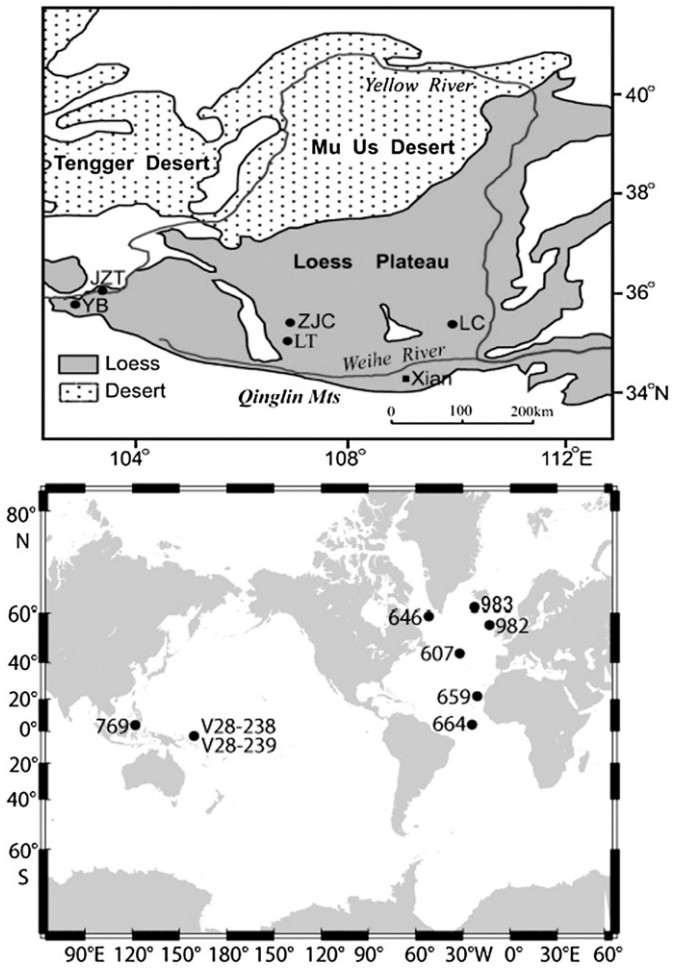

Fig. 1. Upper panel: map of the distribution of the cited loess profiles from the Chinese loess plateau, including Zhaojiachuan (ZJC), Lingtai (LT), Jiuzhoutai (JZT), Yuanbao (YB), and Luochuan (LC). Lower panel: map with location of the 9 marine sediment cores from which data are considered in this study.

solely by delayed PDRM acquisition due to surficial mixing associated with bioturbation and physical disturbance by wind on the Chinese Loess Plateau because mixing is generally confined to the uppermost sediment layer. In contrast, such displacements could result from delayed CRM acquisition. Spassov et al. (2003) assumed that CRM acquisition could occur well below the point where a PDRM is completely locked-in. This model requires that the NRM will be completely contaminated by the CRM carried by neoformed pedogenic single domain maghemite particles and that neither thermal nor AF demagnetization will be able to separate this CRM from a PDRM. However, previous studies indicate that the characteristic remanent magnetization (ChRM) of samples that cross the MBB is dominated by magnetite rather than by maghemite, which indicates that detrital particles dominate the ChRM (Zhu et al., 1994). In addition, loess unit L8 underlies a well-developed paleosol unit S7; the warm period associated with formation of S7 had little effect on the underlying loess unit except in the material immediately below the paleosol due to the downward propagation of pedogenesis (Zhu et al., 1994). The required deep CRM acquisition process proposed by Spassov et al. (2003) is therefore unlikely for the Chinese loess.

Liu et al. (2005) correlated two adjacent Chinese loess profiles at Yuanbao and Jiuzhoutai in a region that is minimally affected by pedogenesis (Fig. 1). They used a range of parameters and found that strong susceptibility peaks recorded at Yuanbao were not developed at Jiuzhoutai because the average annual precipitation at Jiuzhoutai is lower than at Yuanbao. More recently, Wang et al. (2006) compared the position of the MBB in different Chinese loess profiles, and found it either at the base of L8 or in the uppermost part of S8. Tauxe et al. (1996) proposed that variable positions of the MBB reflect complexities associated with NRM acquisition in the Chinese loess. In contrast, Wang et al. (2006) attributed the complicated paleomagnetic behaviour in the Chinese loess to regional and/or local climate (precipitation) variability that produces variable pedogenesis, and therefore variable neoformation of pedogenic magnetic minerals and variably delayed remanence acquisitions, across the Chinese Loess Plateau.

To test whether the variable position of the recorded MBB results from incorrect interpretation of MIS boundaries based on magnetic susceptibility correlations, we use quartz grain size to define paleoclimate boundaries. Quartz is highly resistant to pedogenic alteration, therefore quartz grain size is a useful proxy for Asian winter monsoon intensity (Sun et al., 2006). Similar quartz grain size variations are observed at Lingtai (LT) and Zhaojiachuan (ZJC) across units L8 and S8 (Fig. 2a, b), which permits confident stratigraphic correlation between the two sites. In contrast, magnetic susceptibility profiles have different patterns (Fig. 2c, d), which indicates that changes in local precipitation can cause significant variability in pedogenesis and associated magnetic susceptibility enhancement. Magnetic susceptibility therefore does not enable consistent identification of the authentic positions of paleoclimatic boundaries and should not be used for fine-scale inter-profile correlations in the Chinese loess.

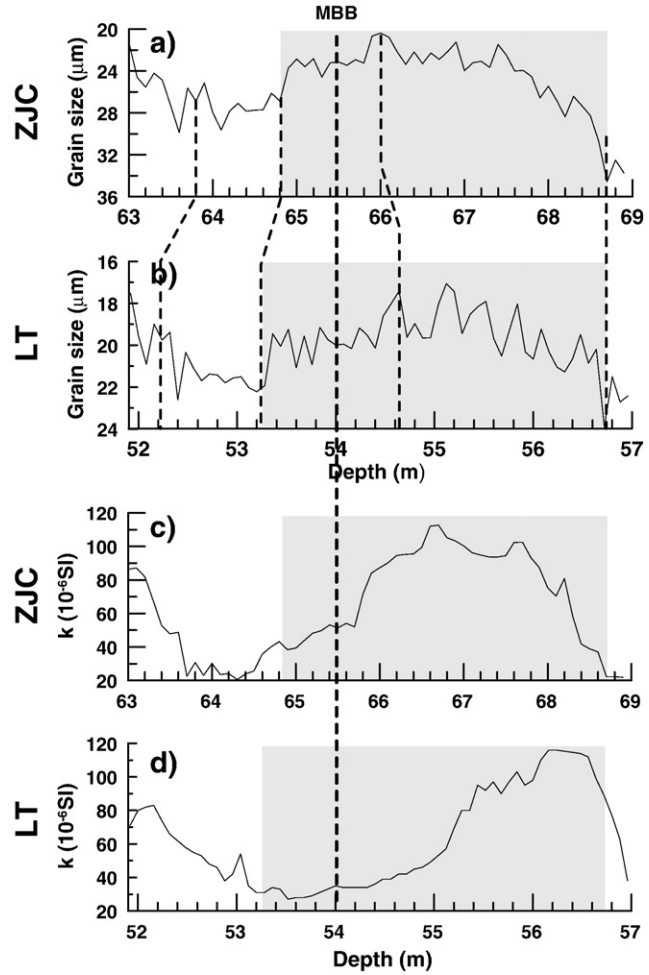

Fig. 2. (a), (b) Profiles of quartz grain size for the Zhaojiachuan (ZJC) and Lingtai (LT) sections, respectively, from the central Chinese Loess Plateau. (c), (d) Magnetic susceptibility profiles for the ZJC and LT sections, respectively. Data are from Sun et al. (2006). The dashed lines mark the positions of the recorded MBB and quartz grain size tie points.

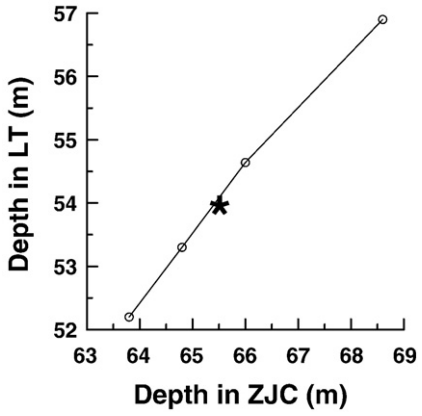

Fig. 3. Correlation of the depths of tie points between the Lingtai (LT) and Zhaojiachuan (ZJC) sections based on variations in quartz grain size. The star indicates the position of the MBB, which is located close to the stratigraphic trend. This suggests that there are no substantial displacements of the MBB for the Chinese loess sequences, probably because of high sedimentation rates and relatively shallow NRM lock-in. Paleomagnetic data are from Sun et al. (2006).

If we use sharp changes in quartz grain size to define glacial–interglacial boundaries, the MBB is consistently observed just below a glacial-interglacial boundary for both loess profiles (Fig. 2), in agreement with the observation of Wang et al. (2006). When the depths of tie points from LT and ZJC are correlated based on variations in quartz grain size (Fig. 3), the position of the MBB falls close to the correlation line. This suggests that there are no substantial displacements in the position of the MBB for these two Chinese loess profiles, probably due to high sedimentation rates and relatively shallow NRM lock-in.

4. Microtektites from the Chinese loess

The strongest evidence for the large lock-in depth suggested by Zhou and Shackleton (1999) stems from a single study of microtektites from a single Chinese loess profile (Li et al., 1993) in which it was assumed that the microtektites are coeval with Australasian marine microtektites. However, no further studies have described the spatial and stratigraphic distribution of microtektites in the Chinese loess. Detailed comparison of the geochemical composition of the loess microtektites indicates that they probably have a different origin than the Australasian microtektites as outlined below. The 14 microtektites reported from above the MBB in loess unit L8 were subdivided by Li et al. (1993) into 4 sub-groups based on their chemical composition (Appendix A). Group 1 has only one sample. Microtektites in group 2 have K_2O contents (>4 wt%) that have never been reported for Australasian microtektites (where K_2O contents are <4 wt%). Samples from group 3 have high Al_2O_3 contents (>30 wt%). Some Australasian microtektites with up to 35 wt% Al_2O_3 have low K_2O contents (<1 wt%) and higher CaO contents (generally >4 wt%). These compositions are not compatible with the chemical composition of loess microtektite group 3. The compositions of loess microtektite group 4 are similar to olivine, which does not resemble the Australasian marine microtektites. In summary, none of the Chinese loess microtektites have compositions comparable to those of the Australasian marine microtektites (Glass and Koeberl, 2006). This indicates that the Chinese loess microtektites have a different origin from the Australasian microtektites. This conclusion is supported by the fact that the Chinese microtektites occur well above the MBB, whereas the Australasian microtektites occur well below the MBB. We therefore suggest that these microtektites are not reliable markers for correlating Chinese loess and marine sediment records.

5. Position of the MBB in marine sediments

We exclude many of the cores used in previous analyses of MBB lock-in for reasons stated above (see Section 2). In addition to these exclusions of ODP holes 609, 660A, 665A, 804C, and 807A, we also exclude data from DSDP Hole 502B, and ODP holes 758A and 851E (Tauxe et al., 1996) because of an insufficient number of $\delta^{18}O$ data points in these data sets. It has been suggested that the NRM at DSDP Hole 552A may have been seriously distorted by coring (Tauxe et al., 1996). This record is therefore not used here. ODP Site 610 is excluded

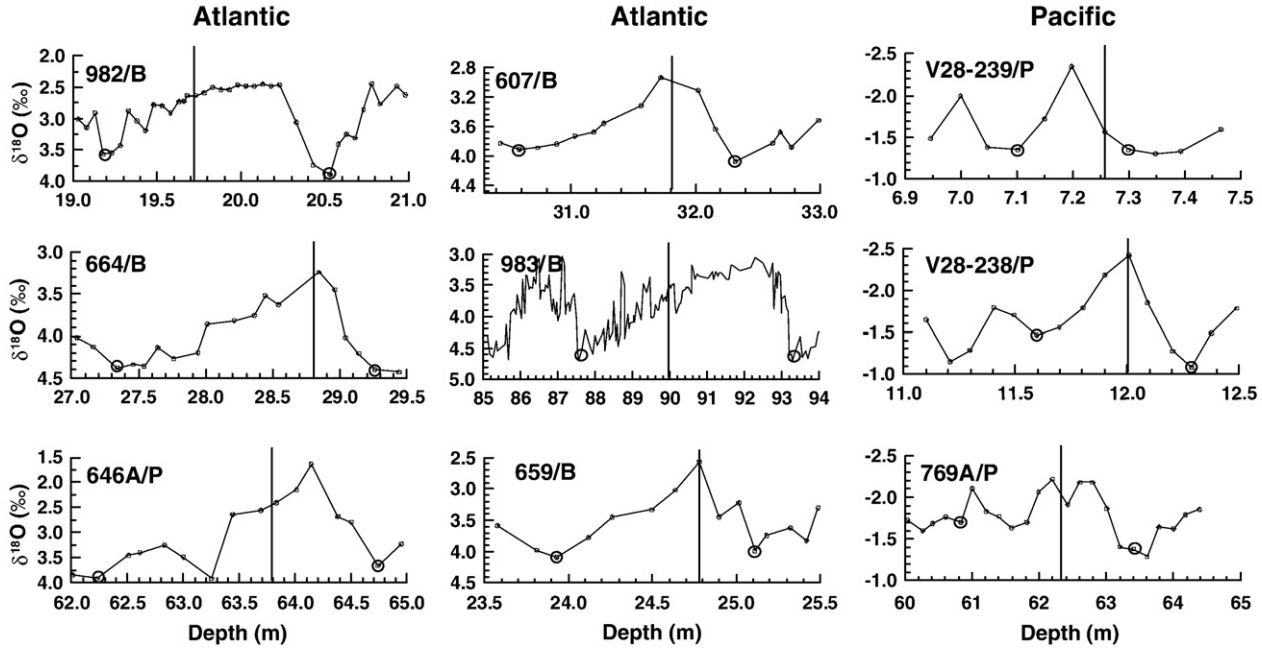

Fig. 4. Oxygen isotope records plotted versus depth for a global compilation of marine MBB records with good quality $\delta^{18}O$ data. The solid lines mark the respective stratigraphic positions of the MBB. B and P indicate whether the $\delta^{18}O$ records are from benthic or planktonic foraminifera, respectively. The large open circles indicate the age tie points, which correspond to MIS18.4 and 20.2, respectively. See Table 1 for data sources.

Table 1
Site information for the cores discussed in this paper

Core	Latitude	Longitude	Water depth (m)	SAR (cm/kyr)	Type of $\delta^{18}O$ data	Reference
ODP 607A	42°N	33°W	3427	4.1	Benthic	Ruddiman et al. (1989), Clement and Kent (1986)
ODP 646A (cd)	58°N	48°W	3451	8.6	Planktonic	Aksu et al. (1989)
ODP 659A (cd)	18°N	21°W	3070	3.1	Benthic	Tiedemann et al. (1994), Tauxe et al. (1989)
ODP 664B (cd)	0°N	23°W	3806	3.7	Benthic	Tauxe et al. (1989, 1996)
ODP 769A (cd)	9°N	121°E	3645	11.0	Planktonic	Linsley and Dunbar (1994), Schneider et al. (1992)
ODP 982C (cd)	58°N	16°W	1135	2.8	Benthic	Venz et al. (1999), Channell and Guyodo (2004)
ODP 983A (cd)	61°N	336°E	1983	~15	Benthic	Channell and Kleiven (2000), Kleiven et al. (2003)
V28-238 (mbsf)	1°N	161°E	3120	1.6	Planktonic	Shackleton and Opdyke (1973)
V28-239 (mbsf)	3°N	159°E	3490	1.0	Planktonic	Shackleton and Opdyke (1973, 1976)

cd and mbsf represent composite depth and m below seafloor depth scales, respectively, which are used for plotting the data presented in this paper. SAR = sediment accumulation rate. The SAR stated for ODP Hole 983A is estimated here as the value in the immediate vicinity of the MBB.

because it has a large uncertainty (more than 50 cm) in the placement of the MBB (Tauxe et al., 1996). Instead, we include two new North Atlantic records from ODP holes 982C (SAR = 1–4 cm/kyr) and 983A (SAR = ~15 cm/kyr). These records complement 7 others that we have compiled (Fig. 4), all of which provide reasonable quality paleomagnetic and $\delta^{18}O$ data across the MBB. The total suite of records that we consider to be suitable for such an analysis includes ODP holes 607A, 646A, 659A, 664B, 769A, 982C, and 983A, and cores V28-238 and V28-239 (Fig. 4). The SAR at these sites ranges from about 1 to 15 cm/kyr (Table 1).

We use two approaches to quantify the effects of surficial mixing and PDRM lock-in. In the first, we compare the relative stratigraphic positions of the MBB and $\delta^{18}O$ tie points. For two adjacent cores from the same hydrographic setting, the ratio of their sedimentation rates through any interval will be more or less constant relative to each other, which will define a linear correlation trend for the $\delta^{18}O$ tie points. If there is no relative MBB displacement, the correlation point for the MBB will fall on the correlation trend defined by the two $\delta^{18}O$ curves. Conversely, the tie point for the MBB will depart from the stratigraphic trend defined by the $\delta^{18}O$ data if mixing and lock-in effects are not negligible. This rationale was used by Sagnotti et al. (2005) to investigate paleomagnetic lock-in from the Gulf of Salerno, Italy.

Cores V28-238 and V28-239 are from a similar hydrographic environment. Correlation of planktonic foraminiferal $\delta^{18}O$ records from the two sites avoids potential phase differences between benthic and planktonic foraminiferal $\delta^{18}O$ records. Correlation of $\delta^{18}O$ records and the observed stratigraphic locations of the MBB between the two sites are shown in Fig. 5. The MBB was recorded at depths of 12.00 m (mid-point of MIS 19) and 7.26 m (lower MIS 19) in cores V28-238 and V28-239, respectively. Such a discrepancy in the stratigraphic position of the MBB suggests that it has been displaced downward to greater depth in core V28-239, due primarily to its lower sedimentation rate (the same mixing depth results in a greater temporal offset for more slowly deposited sediments). It should also be noted that a depth of 7.35 m has often been reported for the position of the MBB for core V28-239, following Shackleton and Opdyke (1973). This position has been used to indicate deep paleomagnetic lock-in for core V28-239. We use a depth of 7.26 m for the MBB in core V28-239, as indicated by Shackleton and Opdyke (1976). It appears that the MBB position reported by Shackleton and Opdyke (1973) was a typographical error (D.V. Kent, personal communication, 2008), which was correctly stated by Shackleton and Opdyke (1976).

Assuming that the depth offset (L) of the MBB for these two sites is comparable, we get:

$$(X^*-X_1-L)/(Y^*-Y_1-L) = (X_2-X_1)/(Y_2-Y_1), \quad (1)$$

where * denotes the MBB and the numbers denote $\delta^{18}O$ tie points. X and Y represent the depths of the tie points in cores V28-238 and V28-239, respectively (Fig. 5c). Based on Eq. (1), L is estimated to be 8.4 cm for both cores. Thus, the corrected position for the MBB will be at 11.92 m and 7.18 m in cores V28-238 and V28-239, respectively. The paleomagnetic record for core V28-239 was considered by Tauxe et al. (1996) to suffer from a similar affliction as nearby ERDC103p, where thermal demagnetization revealed an overprint that caused a

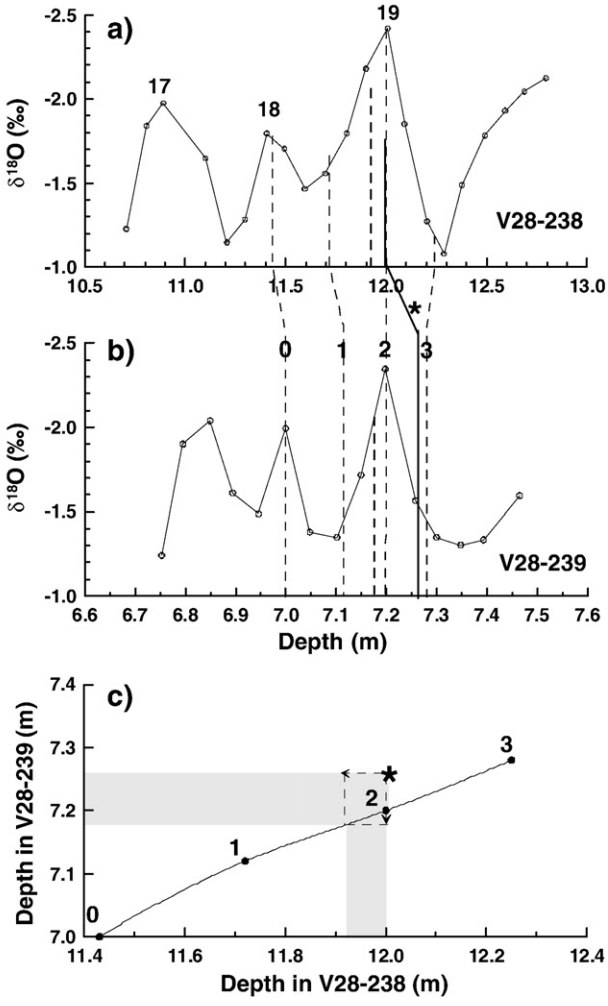

Fig. 5. Correlation of planktonic $\delta^{18}O$ data between cores: (a) V28-238 and (b) V28-239 (from Shackleton and Opdyke (1973, 1976)). The thick line marked with a star indicates the measured positions of the MBB. The thin dashed lines with numbers indicate the $\delta^{18}O$ tie points. The thick dashed lines indicate the corrected positions of the MBB by upward shifting with L = 8.4 cm. (c) Correlation of the $\delta^{18}O$ tie points (solid circles) and the MBB (star) between cores V28-238 and V28-239. The thick arrow indicates that the stratigraphic locations of the MBB for these two sites should be shifted upward by 8.4 cm (marked by the shading and the dashed arrows) to match the stratigraphic trend defined by the $\delta^{18}O$ correlation points.

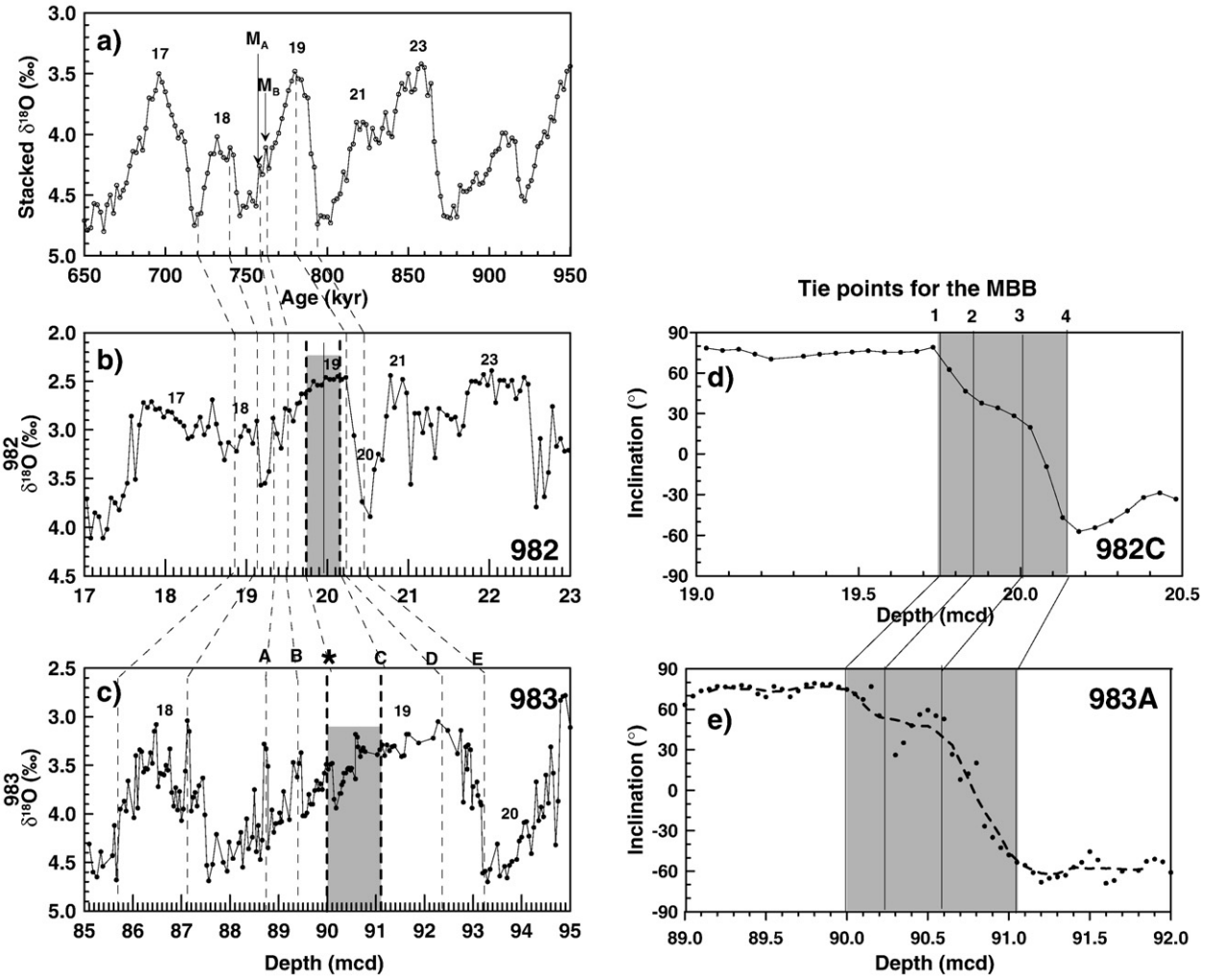

Fig. 6. Comparison of benthic oxygen isotope records around MIS 19 for: (a) a stacked global benthic δ^{18}O record (Lisiecki and Raymo, 2005) with benthic δ^{18}O data from sites (b) 982 (Venz et al., 1999), and (c) 983 (Channell and Kleiven, 2000), respectively. (d), (e) Depth plots of paleomagnetic inclination variations for holes 982C and 983A, respectively. The shaded areas in (b)–(e) mark the measured MBB transition intervals. Dashed lines (A–E) indicate δ^{18}O tie points. In (a), MA and MB are two δ^{18}O minima that are recorded before the termination of MIS 19. In (e), the dashed curve represents a 7-point smoothing of the inclination data, while the solid circles represent the raw data. The lines denoted as 1–4 in (d) and (e) indicate the tie points for the MBB transition recorded from Hole 982C and the smoothed trend for the record from Hole 983A.

downward shift in the MBB. Questions concerning the quality of paleomagnetic data in this core, and the 9 cm discrepancy in the reported location of the MBB in two successive studies of core V28-239 (Shackleton and Opdyke, 1973, 1976), therefore mean that our estimated MBB depth offset of ~8.4 cm should be treated with caution.

The same procedure can be applied to the benthic foraminiferal δ^{18}O records across the paleomagnetically well-defined MBB for ODP holes 982C and 983A (Fig. 6a–c) (Venz et al., 1999; Channell and Kleiven, 2000). The higher sedimentation rates for these sites compared to sites V28-238 and V28-239 mean that they have recorded more details of transitional field behaviour during the MBB. However, some high-frequency features recorded in Hole 983A are not observed in Hole 982C. This unambiguously indicates smoothing associated with lock-in processes in Hole 982C (Channell and Guyodo, 2004). To link the MBB transition zone between holes 982C and 983A, paleomagnetic inclinations for Hole 983A were smoothed using a seven-point averaging, which produces a clear correlation (Fig. 6d, e). Rather than estimating a single value of L, as was done for sites V28-238 and V28-239, four displacement values were estimated for four tie points within the MBB transition (Fig. 6d, e; denoted as 1 to 4 in Fig. 7). The average downward displacement of the MBB for holes 982C and 983A is 23 ± 6 cm, which is consistent with

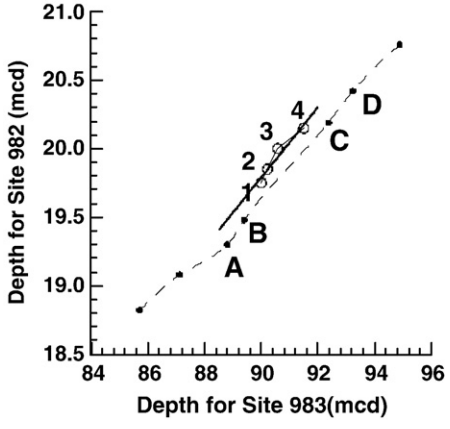

Fig. 7. Correlation of the stratigraphic tie points for ODP sites 982 and 983 (from Fig. 6). The open circles with numbers indicate the tie points from within the measured MBB transition interval. The solid circles with letters indicate the δ^{18}O tie points. The dashed curve represents the stratigraphic trend of δ^{18}O tie points, and the thick line represents the stratigraphic trend of the points from the MBB transition. Apparently, relative to Site 983, the MBB transition has been systematically displaced downward at Site 982. The nearly parallel trend between the MBB and δ^{18}O tie points suggests that the effects of the downward displacements caused by the SML and lock-in processes are comparable for the tie points (1–4) from the MBB transition.

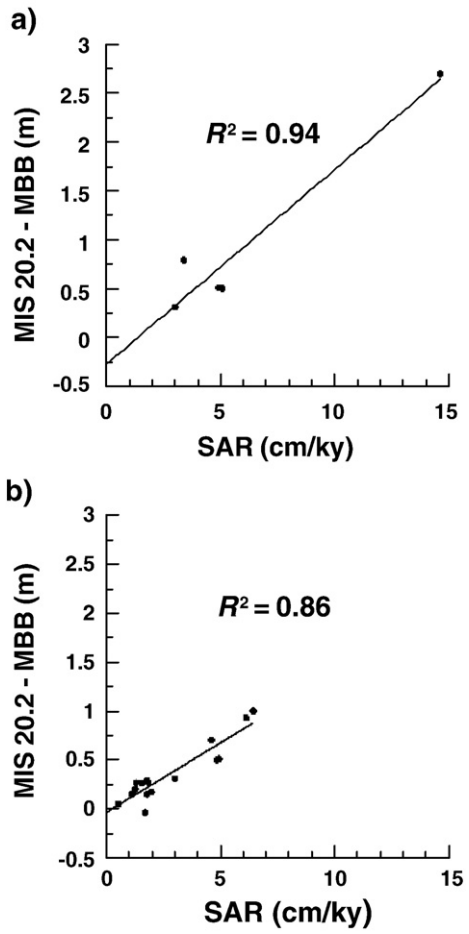

Fig. 8. Plot of the depth difference between MIS 20.2 and the MBB versus the sediment accumulation rate (SAR). (a) Data for ODP holes 607A, 659A, 664B, 982C, and 983A, from which benthic foraminiferal $\delta^{18}O$ data are available; and (b) data from the analysis of Tauxe et al. (1996) who used mixed paleoclimate proxies; SAR is calculated based on the identification of MIS 18.4 (753 kyr) and MIS 20.2 (792 kyr) in the respective cores. The estimated downward displacements of the MBB are: (a) about 27 cm and (b) 0, respectively.

a local ~20 cm SML thickness (Thomson et al., 2000). Tauxe et al. (2006) argued that the ODP Hole 983A $\delta^{18}O$ record could have been shifted relative to the MBB because of unknown lags when foraminifera were transported along the seafloor before being deposited in the sediment drift at Site 983. This argument is plausible for planktonic foraminifera, but is less applicable to benthic foraminifera that live within sediment. We therefore consider the consistent ~20 cm downward displacement of the MBB for this pair of sites to be a meaningful estimate. This estimate is consistent with the findings of Channell and Guyodo (2004). Nevertheless, further high-resolution paleomagnetic and paired benthic and planktonic foraminiferal $\delta^{18}O$ records are needed from different hydrographic settings to confirm our results.

The second approach that we use to examine PDRM lock-in has been used by deMenocal et al. (1990) and Tauxe et al. (1996). It is less objective than our first approach because it strongly depends on the selected tie points and on whether correlated $\delta^{18}O$ features are really synchronous. The sites used include ODP holes 607A, 659A, 664B, 982C, and 983A from which benthic foraminiferal $\delta^{18}O$ data are available (Fig. 4). First, following Tauxe et al. (1996), we selected MIS 20.2 as a reference point with depth D_1 (Fig. 4). If the observed MBB depth (D_O) with respect to D_1 is shifted below its expected depth (D_E) by L, then:

$$D_O - D_1 = D_E - D_1 - L. \quad (2)$$

We plot ($D_O - D_1$) against SAR, which gives an average downward offset, L, of ~27 cm (Fig. 8a). This estimate is consistent with our first approach. In contrast, the downward displacement of the MBB is almost zero (Fig. 8b) if mixed paleoclimatic proxies are used (Tauxe et al., 1996). The use of mixed paleoclimatic proxies is not desirable for such an analysis, but it should also be noted that our linear regression (R^2 = 0.94) is influenced by the limited data set, by the single data point from ODP Hole 983A with high SAR, and by any errors in estimating the stratigraphic distance between age tie points. It is therefore highly desirable to develop a much more extensive high quality data set to rigorously constrain this problem in future.

6. Discussion

6.1. Correlation of the MBB between marine sediments and the Chinese loess

The well-established presence of a bioturbated SML in most marine environments (Boudreau, 1994, 1998) implies that the negligible MBB depth offset (~1 cm) reported by Tauxe et al. (1996) is unrealistic. We conclude that the analysis of Tauxe et al. (1996) is flawed because of correlation uncertainties due to the use of mixed paleoclimatic proxies. This approach is likely to be compromised by age offsets among different $\delta^{18}O$ records that result from hydrographic differences

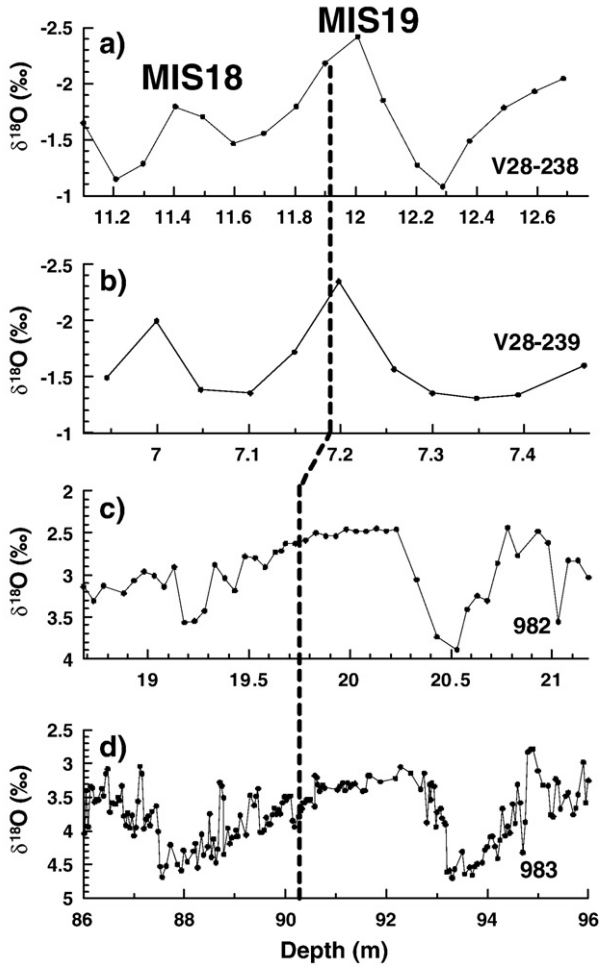

Fig. 9. (a, b) Depth plots of $\delta^{18}O$ for cores V28-238 and V28-239, respectively (from Shackleton and Opdyke, 1973, 1976). (c, d) Depth plots (metres composite depth, or mcd) of $\delta^{18}O$ for ODP sites 982 (Venz et al., 1999) and 983 (Channell and Kleiven, 2000), respectively. The thick dashed line marks the adjusted position of the MBB from this study.

among sites. It should be noted that surficial mixing can also shift $\delta^{18}O$ records to some extent (Bard et al., 1987). Based on the unmixing model of Bard et al. (1987), deMenocal et al. (1990) showed that for most cores with sedimentation rates >1 cm/ka, displacements of $\delta^{18}O$ signals due to surficial mixing are limited (less than several cm).

For North Atlantic ODP holes 982C and 983A, the estimated ~20 cm downward offset of the MBB is consistent with the thickness (10–20 cm) of the SML for sites close to the Rockall Plateau at water depths comparable to those of Site 982 (Thomson et al., 2000). This consistency implies that the downward displacement of the MBB relative to the foraminiferal $\delta^{18}O$ record is dominantly controlled by the SML, which suggests that the PDRM lock-in depth below the SML is small, of the order of only a few cm (Channell and Guyodo, 2004). This potentially shallow lock-in is probably due to flocculation of sediments and inter-granular forces (Tauxe et al., 2006), which are much stronger than the magnetic forces that lead to the post-depositional realignment of magnetic particles that is needed for PDRM acquisition (Katari et al., 2000).

Based on the Chinese loess pedostratigraphy defined using quartz grain size (Fig. 2a, b), the MBB is recorded within interglacial paleosol S8, just below the L8/S8 boundary. The MBB has been widely placed at the mid-point of MIS 19, which has been assigned an age of 780 ka (Tauxe et al., 1996). Our results indicate that the MBB should be recorded just below the MIS 18/19 boundary after correcting for the downward displacements due to the combined effects of lock-in and surficial mixing processes (Fig. 9). Thus, it is reasonable to correlate Chinese loess units L8 and S8 with MIS 18 and MIS 19, respectively, which provides a consistent position for the MBB and resolves a longstanding conundrum. Obtaining a consistent indication of the position of the MBB between marine sediments and the Chinese loess is also important because the North Atlantic region is believed to be teleconnected to the Chinese Loess Plateau (Heller and Liu, 1984, 1986; Kukla et al., 1988; Rohling et al., 2003; Balsam et al., 2005), so that a good correlation would be expected between paleoclimate records from these two regions.

6.2. Uncertainties

We have used two approaches to estimate the depth offset of the MBB in marine sediments. Estimations from the first approach could be misleading because of the small number of records used in our analysis and because of issues that could affect each of the analysed records, as indicated by Tauxe et al. (1996, 2006). In the second approach, which follows the methods used by deMenocal et al. (1990) and Tauxe et al. (1996), linear extrapolation of the regression line between D_O–D_1 and SAR could be invalid for extremely low sedimentation rates. For the small number of records used, individual data points can also have a strong effect on the resulting linear regression. Moreover, there are ambiguities in selecting tie points, and in accurately defining paleoclimatic boundaries. There are also uncertainties concerning the global synchroneity of features in $\delta^{18}O$ records. All of this contributes to uncertainties in estimating the lock-in depth. Although our first approach is based on only two pairs of data (e.g., ODP holes 982C and 983A, and cores V28-238 and V28-239), it uses more tie points to construct a correlation trend. Erroneous selection of tie points will be immediately identified because they will distort the linear correlation trend. Therefore, our first approach is more objective than the second approach.

7. Conclusions

Our analysis indicates that the authentic position of the MBB is in late MIS 19, just below the transition into MIS 18. This conclusion is based on two approaches, which indicate that the MBB has been shifted downward in the studied marine sediment records up to about 20 cm. Our analysis suggests that lock-in processes have smaller effects on PDRM acquisition than surficial mixing due to bioturbation in marine sediments. Considerable future work is needed to develop a high quality global paleomagnetic and oxygen isotopic database for pairs of marine sediment cores from the same hydrographic setting to rigorously constrain understanding of PDRM lock-in.

For the Chinese loess, quartz grain size is a proxy that is insensitive to pedogenesis and is therefore useful for determining the positions of paleoclimate boundaries. The use of quartz grain size yields a late interglacial position for the MBB within the upper part of paleosol unit S8. This is consistent with marine records where the MBB is recorded in MIS 19, although the exact downward displacement of the MBB in marine records still needs further study. This interpretation suggests that MIS 18 and 19 correlate with loess and paleosol units L8 and S8, respectively. This solution successfully avoids an exceptionally large, and difficult to explain, lock-in depth (2–3 m) for the MBB in Chinese loess sequences and is fully compatible with a modern understanding of pedogenic processes in loess sequences.

Acknowledgments

This work was supported by the European Commission through a Marie Curie Fellowship (proposal #7555), by the Bairen Program of the Chinese Academy of Sciences and by NSFC grant 40221402. We have benefited from discussions with L. Tauxe, D. Kent, J. Channell and M. Raymo. We thank J. Channell, K. Kleiven and M. Raymo for providing data and L. Tauxe, F. Florindo, M. Delaney and an anonymous reviewer for helpful comments that improved the paper.

Appendix A. Geochemical composition of microtektites in Chinese loess (from Li et al., 1993)

Group 1							
SiO_2				85.03			
Al_2O_3				9.13			
FeO				2.39			
MgO				0.55			
CaO				0			
Na_2O				0.37			
K_2O				2.09			
TiO_2				0.44			
Group 2		Loess-1		Loess-2		Loess-3	
SiO_2		53.28		54.54		46.92	
Al_2O_3		17.1		17.28		12.18	
FeO		10.71		9.42		9.11	
MgO		7.77		7.74		5.84	
CgO		1		0.46		0.11	
Na_2O		0		1.58		0.02	
K_2O		8.67		7.66		8.96	
TiO_2		1.46		0.23		–	
Group 3	L-1	L-2	L-3	L-4	L-5	L-6	L-7
SiO_2	53.94	40.93	45.18	48.91	50.07	49.37	54.28
Al_2O_3	40.4	57.37	30.01	31.28	35.75	30.14	38.14
FeO	1.67	0.62	2.16	3.72	1.22	5.72	2.97
MgO	0.73	0	2.19	3.53	1.61	4.53	1.37
CaO	0.64	0.2	0.15	0.07	0.71	0	0.09
Na_2O	0	0.6	0.15	0.22	3.11	1.74	1.18
K_2O	0.57	0.28	8.9	9.61	7.34	8.5	0.57
TiO_2	0.37	0	0.49	0	0.2	0	0
Group 4		L-8		L-9		L-10	
SiO_2		46.48		51.08		47.51	
Al_2O_3		0.59		1.3		0.46	
FeO		1.25		0.71		2.21	
MgO		45.93		44.84		47	
CaO		0.08		0.45		0.02	
Na_2O		0.04		1.45		0.07	
K_2O		0		0.17		0.02	
TiO_2		0		0		0.02	

Sample numbers are those of Li et al. (1993).

References

Aksu, A.E., de Vernal, A., Mudie, P., 1989. High-resolution foraminifer, palynologic and stable isotopic records of upper Pleistocene sediments from the Labrador Sea: paleoclimatic and paleoceanographic trends. Proc. Ocean Drill. Prog., Sci. Results 105, 167–185.

Balsam, W., Ellwood, B., Ji, J.F., 2005. Direct correlation of the marine oxygen isotope record with the Chinese Loess Plateau iron oxide and magnetic susceptibility records. Palaeogeogr. Palaeoclimatol. Palaeoecol. 221, 141–152.

Bard, E., Arnold, M., Duprat, J., Moyes, J., Duplessy, J.-C., 1987. Reconstruction of the last deglaciation: deconvolved records of O-18 profiles, micropaleontological variations and accelerator mass spectrometric 14-C dating. Clim. Dyn. 1, 101–112.

Bleil, U., von Dobeneck, T., 1999. Geomagnetic events and relative paleointensity records—clues to high-resolution paleomagnetic chronostratigraphies of Late Quaternary marine sediment? In: Fischer, G., Wefer, G. (Eds.), Use of Proxies in Paleoceanography: Examples from the South Atlantic. Springer-Verlag, Berlin, pp. 635–654.

Boudreau, B.P., 1994. Is burial velocity a master parameter for bioturbation? Geochim. Cosmochim. Acta 58, 1243–1249.

Boudreau, B.P., 1998. Mean mixed depth of sediments: the wherefore and the why. Limnol. Oceanogr. 43, 524–526.

Channell, J.E.T., Guyodo, Y., 2004. The Matuyama Chronozone at ODP Site 982 (Rockall Bank): evidence for decimeter-scale magnetization lock-in depths. AGU Geophys. Monogr. Ser. 145, 205–219.

Channell, J.E.T., Kleiven, H.F., 2000. Geomagnetic palaeointensities and astrochronological ages for the Matuyama–Brunhes boundary and the boundaries of the Jaramillo Subchron: palaeomagnetic and oxygen isotope records from ODP Site 983. Philos. Trans. R. Soc. Lond., A 358, 1027–1047.

Clement, B., Kent, D., 1986. Geomagnetic polarity transition records from five hydraulic piston core sites in the North Atlantic. Init. Rept. DSDP.

deMenocal, P.B., Ruddiman, W.F., Kent, D.V., 1990. Depth of post-depositional remanence acquisition in deep-sea sediments: a case study of the Brunhes–Matuyama reversal and oxygen isotopic Stage 19.1. Earth Planet. Sci. Lett. 99, 1–13.

Forster, T., Heller, F., 1994. Loess deposits from the Tajik depression (Central Asia): magnetic properties and paleoclimate. Earth Planet. Sci. Lett. 128, 501–512.

Glass, B.P., Koeberl, C., 2006. Australasian microtektites and associated impact ejecta in the South China Sea and the Middle Pleistocene supereruption of Toba. Meteorit. Planet. Sci. 41, 305–326.

Guo, B., Zhu, R., Florindo, F., Pan, Y., Yue, L., 2001. Pedogenesis affecting the Matuyama–Brunhes polarity transition recorded in Chinese loess? Chin. Sci. Bull. 46, 975–981.

Heller, F., Liu, T.S., 1984. Magnetism of Chinese loess deposits. Geophys. J. R. Astron. Soc. 77, 125–141.

Heller, F., Liu, T.S., 1986. Paleoclimatic and sedimentary history from magnetic susceptibility of loess in China. Geophys. Res. Lett. 13, 1169–1172.

Heller, F., Meili, B., Wang, J.D., Li, H.M., Liu, T.S., 1987. Magnetization and sedimentation history of loess in the central loess plateau of China. In: Liu, T.S. (Ed.), Aspects of Loess Research. China Ocean Press, Beijing, pp. 147–163.

Heslop, D., Langereis, C.G., Dekkers, M.J., 2000. A new astronomical time scale for the loess deposits of Northern China. Earth Planet. Sci. Lett. 184, 125–139.

Hyodo, M., 1984. Possibility of reconstruction of the past geomagnetic field from homogeneous sediments. J. Geomagn. Geoelectr. 36, 45–62.

Katari, K., Tauxe, L., King, J., 2000. A reassessment of post-depositional remanent magnetism: preliminary experiments with natural sediments. Earth Planet. Sci. Lett. 183, 147–160.

Kent, D.V., 1973. Post-depositional remanent magnetization in deep-sea sediment. Nature 246, 32–34.

Kleiven, H.F., Jansen, E., Curry, W.B., Hodell, D.A., Venz, K., 2003. Atlantic Ocean thermohaline circulation changes on orbital to suborbital timescales during the mid-Pleistocene. Paleoceanography 18 (PA1008). doi:10.1029/2001PA000629.

Kukla, G., An, Z., 1989. Loess stratigraphy in central China. Paleogeogr. Paleoclimatol. Paleoecol. 72, 203–225.

Kukla, G., Heller, F., Liu, X.M., Xu, T.C., Liu, T.S., An, Z.S., 1988. Pleistocene climates in China dated by magnetic susceptibility. Geology 16, 811–814.

Li, C.L., Yang, Z.Y., Liu, T.S., An, Z.S., 1993. Microtektites and glassy microspherules in loess—their discoveries and implications. Sci. China B36, 1141–1152.

Linsley, B., Dunbar, R., 1994. The Late Pleistocene history of surface water δ^{13}C in the Sulu Sea—possible relationship to Pacific deepwater δ^{13}C changes. Paleoceanography 9, 317–340.

Lisiecki, L., Raymo, M.E., 2005. A Pliocene–Pleistocene stack of 57 globally distributed benthic δ^{18}O records. Paleoceanography 20 (PA1003). doi:10.1029/2004PA001071.

Liu, Q.S., Banerjee, S.K., Jackson, M.J., Deng, C.L., Pan, Y.X., Zhu, R.X., 2005. Inter-profile correlation of the Chinese loess/paleosol sequences during marine oxygen isotope stage 5 and indications of pedogenesis. Quat. Sci. Rev. 24, 195–210.

Roberts, A.P., Winklhofer, M., 2004. Why are geomagnetic excursions not always recorded in sediments? Constraints from post-depositional remanent magnetization lock-in modeling. Earth Planet. Sci. Lett. 227, 345–359.

Rohling, E.J., Mayewski, P.A., Challenor, P., 2003. On the timing and mechanism of millennial-scale climate variability during the last glacial cycle. Clim. Dyn. 20, 257–267.

Ruddiman, W., Raymo, M., Martinson, D., Clement, B., Backman, J., 1989. Pleistocene evolution: northern hemisphere ice sheets and North Atlantic Ocean. Paleoceanography 4, 353–412.

Sagnotti, L., Budillon, F., Dinarès-Turell, J., Iorio, M., Macrì, P., 2005. Holocene sequence from the Salerno Gulf (Italy): implications for "high-resolution" paleomagnetic dating. Geochem. Geophys. Geosyst. 6 (Q11013). doi:10.1029/2005GC001043.

Schneider, D., Kent, D., Mello, G., 1992. A detailed chronology of the Australasian impact event, the Brunhes–Matuyama geomagnetic polarity reversal and global climate change. Earth Planet. Sci. Lett. 111, 395–405.

Shackleton, N.J., Opdyke, N., 1973. Oxygen isotope and paleomagnetic stratigraphy of equatorial Pacific core V28-238: oxygen isotope measurements and ice volumes on a 10^5 to 10^6 year scale. Quat. Res. 3, 39–55.

Shackleton, N.J., Opdyke, N., 1976. Oxygen isotope and paleomagnetic stratigraphy of Pacific core V28-239 Late Pliocene to Latest Pliocene. In: Cline, R.M., Hays, J.D. (Eds.), Investigations of Late Quaternary Paleoceanography and Paleoclimatology. Geol. Soc. Am. Mem., vol. 145, pp. 449–464.

Shackleton, N.J., Hall, M.A., Vincent, E., 2000. Phase relationships between millennial-scale events 64,000–24,000 years ago. Paleoceanography 15, 565–569.

Skinner, L.C., Shackleton, N.J., 2005. An Atlantic lead over Pacific deep-water change across Termination I: implications for the application of the marine isotope stage stratigraphy. Paleoceanography 24, 571–580.

Spassov, S., Heller, F., Evans, M.E., Yue, L.P., von Dobeneck, T., 2003. A lock-in model for the complex Matuyama–Brunhes boundary record of the loess/paleosol sequence at Lingtai (Central Chinese Loess Plateau). Geophys. J. Int. 155, 350–366.

Sun, Y.B., Clemens, S.C., An, Z.S., Yu, Z.W., 2006. Astronomical timescale and palaeoclimatic implication of stacked 3.6-Myr monsoon records from the Chinese Loess Plateau. Quat. Sci. Rev. 25, 33–48.

Tauxe, L., Valet, J., Bloemendal, J., 1989. The magnetostratigraphy of Leg 108 APC Cores. Proc. Ocean Drill. Prog., Sci. Results 108, 865–880.

Tauxe, L., Herbert, T., Shackleton, N.J., Kok, Y.S., 1996. Astronomical calibration of the Matuyama–Brunhes boundary: consequences for magnetic remanence in marine carbonates and the Asian loess sequences. Earth Planet. Sci. Lett. 140, 133–146.

Tauxe, L., Steindorf, J.L., Harris, A., 2006. Depositional remanent magnetization: toward an improved theoretical and experimental foundation. Earth Planet. Sci. Lett. 244, 515–529.

Thomson, J., Brown, L., Nixon, S., Cook, G.T., McKenzie, A.B., 2000. Bioturbation and Holocene sediment accumulation fluxes in the northeast Atlantic Ocean (Benthic Boundary Layer experiment sites). Mar. Geol. 169, 21–39.

Tiedemann, R., Sarnthein, M., Shackleton, N.J., 1994. Astronomic timescale for the Pliocene Atlantic δ^{18}O and dust flux records of Ocean Drilling Program site 659. Paleoceanography 9, 619–638.

Venz, K.A., Hodell, D.A., Stanton, C., Warnke, D.A., 1999. A 1.0 Myr record of glacial North Atlantic intermediate water variability from ODP Site 982 in the northeast Atlantic. Paleoceanography 14, 42–52.

Verosub, K.L., 1977. Depositional and post-depositional processes in the magnetization of sediments. Rev. Geophys. Space Phys. 15, 129–143.

Wang, X.S., Yang, Z.Y., Løvlie, R., Sun, Z.M., Pei, J.L., 2006. A magnetostratigraphic reassessment of correlation between Chinese loess and marine oxygen isotope records over the last 1.1 Ma. Phys. Earth Planet. Inter. 159, 109–117.

Zheng, H.B., An, Z.S., Shaw, J., 1992. New contributions to Chinese Plio–Pleistocene magnetostratigraphy. Phys. Earth Planet. Inter. 70, 146–153.

Zhou, L.P., Shackleton, N.J., 1999. Misleading positions of geomagnetic reversal boundaries in Eurasian loess and implications for correlation between continental and marine sedimentary sequences. Earth Planet. Sci. Lett. 168, 117–130.

Zhu, R.X., Laj, C., Mazaud, A., 1994. The Matuyama–Brunhes and upper Jaramillo transitions recorded in a loess section at Weinan, north-central China. Earth Planet. Sci. Lett. 125, 143–158.

Zhu, R.X., Pan, Y.X., Guo, B., Liu, Q.S., 1998. A recording phase lag between ocean and continent climate changes: constrained by the Matuyama/Brunhes polarity boundary. Chin. Sci. Bull. 43, 1593–1598.